Simple and Convenient Correction of Molecular Dynamics Mechanical Property Predictions for Strain Rate, Temperature, and Degree of Cure

Sagar U. Patil[1], Aaron S. Krieg[1], Leif K. Odegard[1], Upendra Yadav[1], Julia A. King[1], Marianna Maiaru[2], Gregory M. Odegard[1*]

[1]*Michigan Technological University, Houghton, MI-49931, USA*
[2]*University of Massachusetts, Lowell, MA-01854, USA*
[*]*Corresponding author: gmodegar@mtu.edu*

ABSTRACT

It is well-known that all-atom molecular dynamics (MD) predictions of mechanical properties of thermoset resins suffer from multiple accuracy issues associated with their viscous nature. The nanosecond simulation times of MD simulations do not allow for the direct simulation of the molecular conformational relaxations that occur under laboratory time scales. This adversely affects the prediction of mechanical properties at realistic strain rates, intermediate degrees of cure, and elevated temperatures. An efficient method of correcting such MD predictions of elastic properties is proposed and demonstrated. The phenomenological approach is used to correct the predictions of Young's modulus and Poisson's ratio for a DGEBF/DETDA epoxy system for intermediate degrees of cure and temperatures above and below the glass transition temperature. The approach uses characterization data from dynamical mechanical analysis temperature sweep experiments. The mathematical formulation and experimental characterization of the correction is described, and the resulting corrections to the predicted elastic properties for various degrees of cure and temperatures are compared with experiment. This correction is particularly important to mitigate the strain-rate effect associated with MD predictions, as well as to accurately correct predicted mechanical properties at elevated temperatures and intermediate degrees of cure to facilitate accurate and efficient composite material process modeling.

1.   Introduction

Thermosetting polymer composites are extensively used in the aerospace industry because of their relatively low mass density and unique combination of mechanical, thermal, and electrical properties. Computationally-driven design of new generations of thermoset composites for improved performance requires multiscale modeling techniques that are powerful and reliable. Such multiscale modeling must be able to incorporate molecular-scale structure for the prediction of structural-level properties. In particular, molecular dynamics (MD) methods need to be developed that can efficiently predict accurate properties of thermoset neat resins as input into higher-length scale modeling techniques.

Thermoset neat resins consist of a complex network of covalently-linked molecular segments. Generally, for a given state of external conditions (e.g. temperature, mechanical deformation) these segments change their conformation to reach a state of lower energy (relaxation), which ultimately manifests itself as the phenomena known as physical aging and viscoelasticity [1]. These relaxation processes can occur over a wide range of time periods spanning nanoseconds to years, but a significant portion of them occur over timescales associated with composite laminate processing and laboratory mechanical testing. Although all-atom MD simulations have been used over the last several decades to predict molecular structure and nano-scale properties of thermoset resins [2-15], these simulations can only capture the thermoset network

1

response over a nanosecond time scale, creating a significant discrepancy between simulated and laboratory timescales. Although coarse-grain simulation techniques [16-20] can be used to somewhat avert the time scale limitation, some of the fine (and perhaps critically important) details of atomic interactions are lost during coarse-grain simulations.

Because of the timescale discrepancy between the conformational response on laboratory and MD-based timescales, all-atom MD predictions cannot precisely capture the relaxation processes that occur over time increments above nanoseconds. This shortcoming manifests itself in three major ways. First, MD predictions of fully crosslinked thermosets slightly overestimate the room-temperature elastic properties and yield strength [7-9]. This is commonly referred to as the "strain rate effect". Second, MD predictions of mechanical properties above the glass transition temperature (T_g) significantly overestimate experimental observations. Whereas the measurements indicate a multiple order-of-magnitude drop in elastic modulus relative to room temperature [21], simulations predict only about a 50% drop [21]. Third, MD predictions of partially-crosslinked epoxies indicate a steady increase in elastic modulus over the entire range of degrees of cure [8], whereas experiments show a negligible modulus for all levels of crosslinking below the nearly fully-crosslinked state [8, 21]. These three manifestations of the viscous response have the same origin. During simulated mechanical deformations, conformational relaxation processes are not given sufficient time to occur, and thus the associated energy relaxation does not occur, resulting in a stiffer apparent structural response of the network. That is, quantities such as shear modulus and Young's modulus are overpredicted relative to their experimentally-measured values. Decreases in the degree of cure and increases in temperature exaggerate this effect, as they increase the viscous response of the material.

Multiple methods have been proposed to account for the predicted modulus discrepancy in fully crosslinked systems at room temperature [22-26]. However, a convenient and comprehensive approach that accounts for the viscous response of thermosets in MD predictions of mechanical properties for various levels of temperature and degree of cure has not been established. Such a method should have three minimum requirements. First, the method should involve minimal MD simulations. One approach to capturing the viscoelastic effect of polymers in MD predictions is to use a time-temperature superposition principle [11, 24-28]. Approaches like this require significant computational resources to fully characterize each polymer system considered. In a materials engineering environment where computational material design and process optimization need to be performed as efficiently as possible, a full MD-based characterization of the time-temperature superposition is not feasible and does not directly address the dependency of degree of cure on the viscous response. Second, the method should require minimal experimental input. Complete characterization of the material response as a function of strain rate, temperature, and degree of cure can be performed completely by experiment. However, such an approach is prohibitively time-consuming and expensive for most composite material development applications. Third, the method should directly address all three of the above-mentioned manifestations of the viscous response of thermosets.

In this work, a comprehensive approach satisfying all the above-mentioned criteria to establish a phenomenological viscous response correction factor is proposed for elastic properties predicted with all-atom MD simulations. In addition, experimental characterization of thermal and mechanical properties of epoxy for different mixing ratios to efficiently emulate a range of degrees of cure [29, 30] is performed to inform the correction. It is important to emphasize that this correction is phenomenological and is designed to be parameterized by a convenient set of experiments to quickly correct MD predictions for

rapid computationally-driven thermoset material design. It is not intended to be a comprehensive viscoelastic characterization of a resin via classical viscoelastic constitutive modeling [31, 32]. This article is organized as follows: First the methodology to establish the viscous response correction is introduced, followed by a description of the experimental methods used to characterize the correction. The parameterization and optimization of the correction is then described, and results of the modeling with the correction technique follow. The results show that the proposed approach effectively provides an accurate correction for MD predicted Young's moduli of thermosets to capture the effects of strain rate, temperature, and degree of cure.

2. Viscous Correction

Using an approach inspired by the Buckingham π theorem [33], the viscous response can be expressed in terms of a minimal set of dimensionless parameters. It is first assumed that a laboratory-scale mechanical property (specifically, the Young's modulus in this case) can be related to its MD-predicted value by

$$\frac{E}{E_{MD}} = f(\dot{\varepsilon}, \phi, T) \tag{1}$$

where $\dot{\varepsilon}$ is the strain rate, ϕ is the degree of cure, T is the temperature, E is the laboratory-scale Young's modulus, and E_{MD} is the all-atom MD-predicted Young's modulus in the fully crosslinked system at room temperature and MD-scale strain rates. The function f is thus limited to the range of $0 \leq f \leq 1$. The degree of cure is a dimensionless parameter valued between 0 (completely uncured) and 1 (fully cured).

Dimensionless parameters can now be introduced such that this formulation is independent of units and contains functions with direct proportionality with the dependent variable (modulus ratio). Specifically, the following dimensionless variables are defined:

$$\alpha \equiv \frac{\dot{\varepsilon}}{\dot{\varepsilon}_{MD}}, \quad \tau \equiv 1 - \frac{T}{T_r}$$

where $\dot{\varepsilon}_{MD}$ is the strain rate associated with MD time scales (for example, 1×10^8 s^{-1}); T_r is the reference temperature, which should be the highest temperature for which experimental Young's modulus data is available, and herein will be assigned as the processing temperature of the thermoset resin; and T and T_r are expressed in degrees Kelvin. Thus, α and τ are dimensionless scalars that are valued between 0 and 1. Equation (1) can be re-written in terms of the dimensionless parameters

$$\frac{E}{E_{MD}} = f(\alpha, \phi, \tau) \tag{2}$$

For simplicity, Equation (2) can be further specified using a separation-of-variables approach, where $f(\alpha, \phi, \tau)$ is approximated as a product of lower-dimension functions of the independent variables. If we choose the lower-dimension functions to represent the viscous response to strain rate (f_α), degree of cure (f_ϕ), and temperature (f_τ), then such a function could be represented as

$$\frac{E}{E_{MD}} = f_\alpha(\alpha) f_\phi(\phi) f_\tau(\tau, \phi) \tag{3}$$

3

where each of the functions f_α, f_ϕ, and f_τ are directly proportional to their corresponding independent variables, and are valued between 0 and 1. Note that the function associated with temperature, f_τ, is a function of both ϕ and τ because the temperature response (glass transition temperature) of a thermoset is dependent both on temperature and degree of cure. The functional forms and parameters associated with functions in Equation (3) are determined using data from the literature and experiments, as described below.

3. Material

The chosen material for the parameterization of Equation (3) is an epoxy system consisting of a diglycidyl ether bisphenol F (DGEBF) epoxide monomer with a diethyltoluenediamine (DETDA) curing agent, as shown in Figure 1. These materials are commonly marketed as EPON 862 and EPIKURE W, respectively. This system was chosen because it is highly benchmarked and represents a baseline high-performance thermoset.
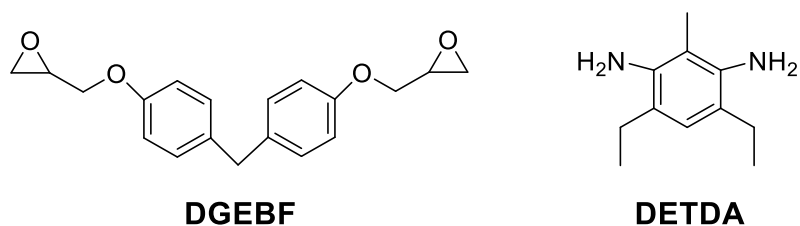
DGEBF   **DETDA**

Figure 1 – DGEBF/DETDA epoxy system molecular structure

4. Experimental details

This section describes the details of the experiments performed to parameterize Equation (3). The experiments were performed on the DGEBF/DETDA epoxy system with a range of mixing ratios as proxies to various degrees of cure [29, 30]. The use of these proxies was necessary because of the high level of difficulty of testing thermal properties of thermoset systems as a function of degree of cure. Although it is acknowledged that the use of off-stoichiometry systems is not a direct substitute for fully stoichiometric systems with intermediate degrees of cure, the proxies provide a reasonable substitute that is relatively easy to fabricate and test.

Epoxy samples were manufactured using a compression molding method. A total of two speedmixer cups were each charged with 50 g of DGEBF epoxy resin and an appropriate amount of DETDA curing agent to achieve systems with seven different mixing ratios of resin and hardener (Table 1). The mixing ratio is defined as the ratio of the mass of the actual DETDA hardener with respect to the mass of the DETDA hardener in the fully stoichiometric mixture. Speedmixer cups were mixed in a FlackTek Speedmixer (DAC 150.1 FVZ) at 2000 rpm for 5 minutes at 25 °C and then heated to 90 °C in a vacuum oven. The speedmixer cups were degassed in the vacuum oven at 90 °C for 30 minutes at 0.101 MPa vacuum pressure. The resin system was cast into a tooling assembly and compression molded at 121 °C for 2 hours and then ramped to 177 °C and held for 2 hours. The compression molder was cooled using air and water until the system was cooled to 150 °C and then was switched to water cooling only to continue cooling the system to 25 °C before removing the plate. The tooling assembly produced 152.4 x 152.4 mm plates with 3.2 mm thickness.

Table 1 – Mixing ratios for DGEBF/DETDA systems

Mixing ratio (%)	DGEBF (g)	DETDA (g)
100	100	26.4
95	100	25.1
85	100	22.4
75	100	19.8
65	100	17.2
55	100	14.5
45	100	11.9

Dynamic mechanical analysis (DMA) was used to determine the thermo-mechanical response of the epoxy as a function of temperature and degree of cure. The testing was performed for all mixing ratios shown in Table 1 to approximate the corresponding degrees of cure. The DMA specimens were cut from fabricated plates using a vertical bandsaw. Three specimens were tested for each mixing ratio. The specimens were 38.1 mm long, 12.7 mm wide, and 3.2 mm thick and the tests were performed using a TA Instruments Q800 DMA in single cantilever test mode with a constant frequency of 1 Hz, an amplitude of 25 μm, and a ramp rate of 3 °C/min. The storage modulus, loss modulus, and tan delta values were continuously monitored during the temperature sweep. The storage modulus for all of the mixing ratios is shown in Figure 2a for the whole range of temperatures. From this data, it is evident that the transition from glassy to rubbery states occurs at decreasing temperatures with decreasing levels of DETDA (thus degree of cure).

Figure 2b shows the storage modulus as a function of mixing ratio at room temperature. It can be seen from the plot that the storage modulus gradually increases from the fully stoichiometric level with decreasing mixing ratios until 65%. This is likely because of increasing levels of mass density of the proxy systems as DETDA monomers are removed. Fully stoichiometric systems with intermediate degrees of cure are not expected to exhibit this behavior, and this is the primary disadvantage of using proxy systems. However, as described below, this behavior did not affect the viscous response parameterization, and the advantages of using proxy systems for the purposes of this study far outweigh this disadvantage. In Figure 2b, it is also observed that as the mixing ratio decreases below 65%, the storage modulus drastically decreases as the sparse network can no longer sustain significant mechanical loads.

The glass transition temperature (T_g) was determined using three different metrics: storage modulus, loss modulus, and tan delta. To determine the T_g using the storage modulus, the onset of the decline in storage modulus was located by finding the intersection between the baseline and the tangent at the point of the highest slope. The T_g values for the loss modulus and tan delta metrics were determined from the peak of the loss modulus and tan delta curves, respectively. Figure 2c shows the T_g values as a function of mixing ratio using all three metrics. It is clear that the T_g trends from the three metrics are very similar with mixing ratio, with only a difference in the magnitude.
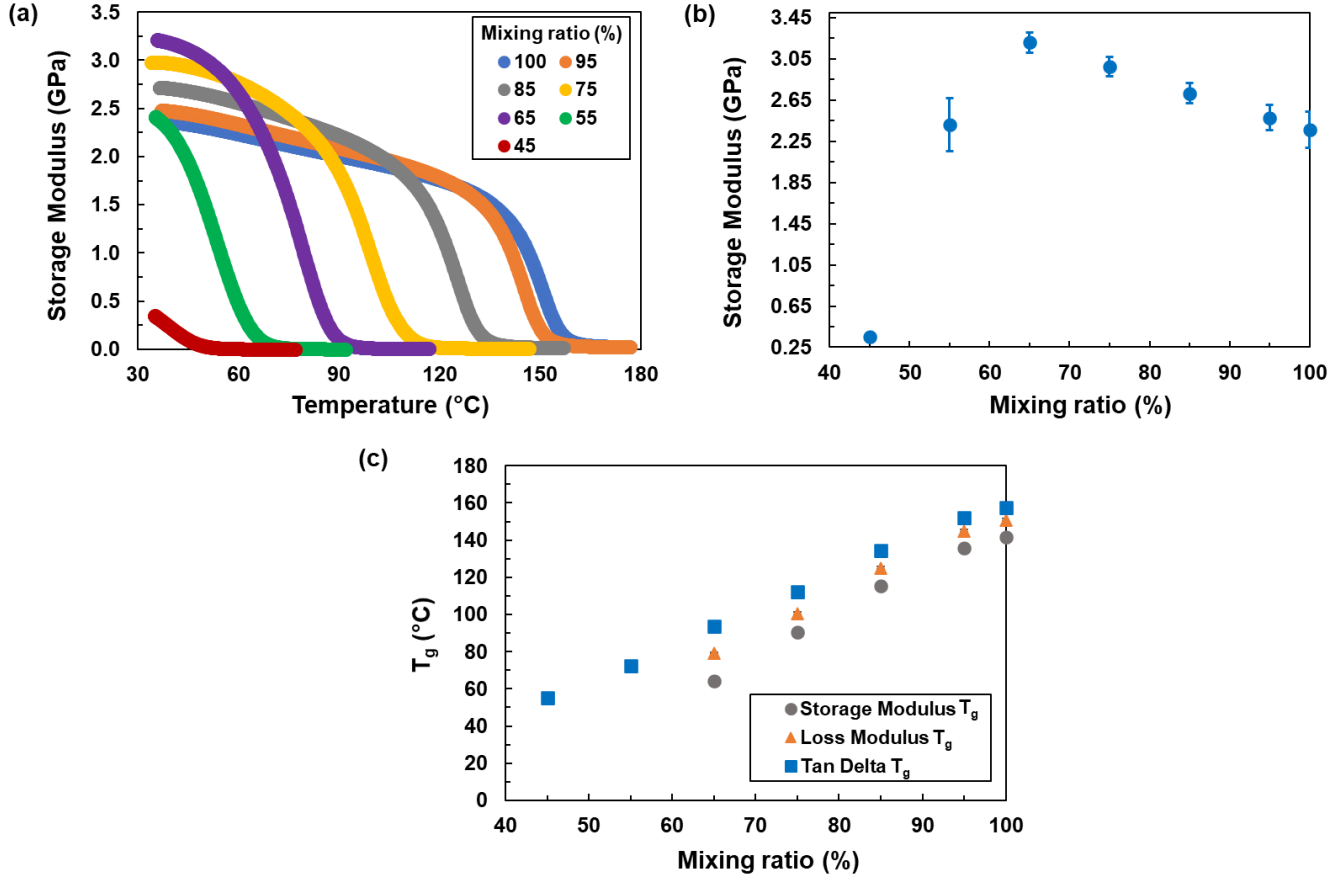
Figure 2 – (a) Representative curves of storage modulus vs temperature, (b) Storage Modulus vs mixing ratio (n=3) at room temperature, (c) T_g vs mixing ratio (n=3, standard deviations are smaller than the symbols)

5. Viscous correction parameterization

The specific forms of functions in Equation 3 and the corresponding phenomenological parameters for the DGEBF/DETDA system were determined as described in this section. First, the specific forms of the functions and the initial guesses of the parameters are outlined, followed by a description of the parameter optimization using the Newton-Raphson [34] iterative numerical technique.

5.1 Functional forms, parameters, and initial guesses

It has been demonstrated [6, 7, 10] that the DGEBF/DETDA system shows a logarithmic dependance of elastic modulus and yield strength on strain rate over a range of strain rates spanning experimental timescales (10^{-5} s^{-1}) to those associated with MD simulations (10^{9} s^{-1}) for fully crosslinked systems at room temperature. Therefore, $f_\alpha(\alpha)$ can be expressed as

$$f_\alpha(\alpha) = \alpha_a ln(\alpha) + \alpha_b \qquad (4)$$

where α_a and α_b are phenomenological parameters. These parameters can be determined by fitting experimental data of the Young's modulus normalized by the modulus predicted by MD (such that $0 \leq f_\alpha \leq 1$) as a function of α. Figure 3 shows such a fit using several experimental data points from the literature [8, 35-37], with dimensionless least-square fitting parameters $\alpha_a = 0.0147$ and $\alpha_b = 1.0849$.
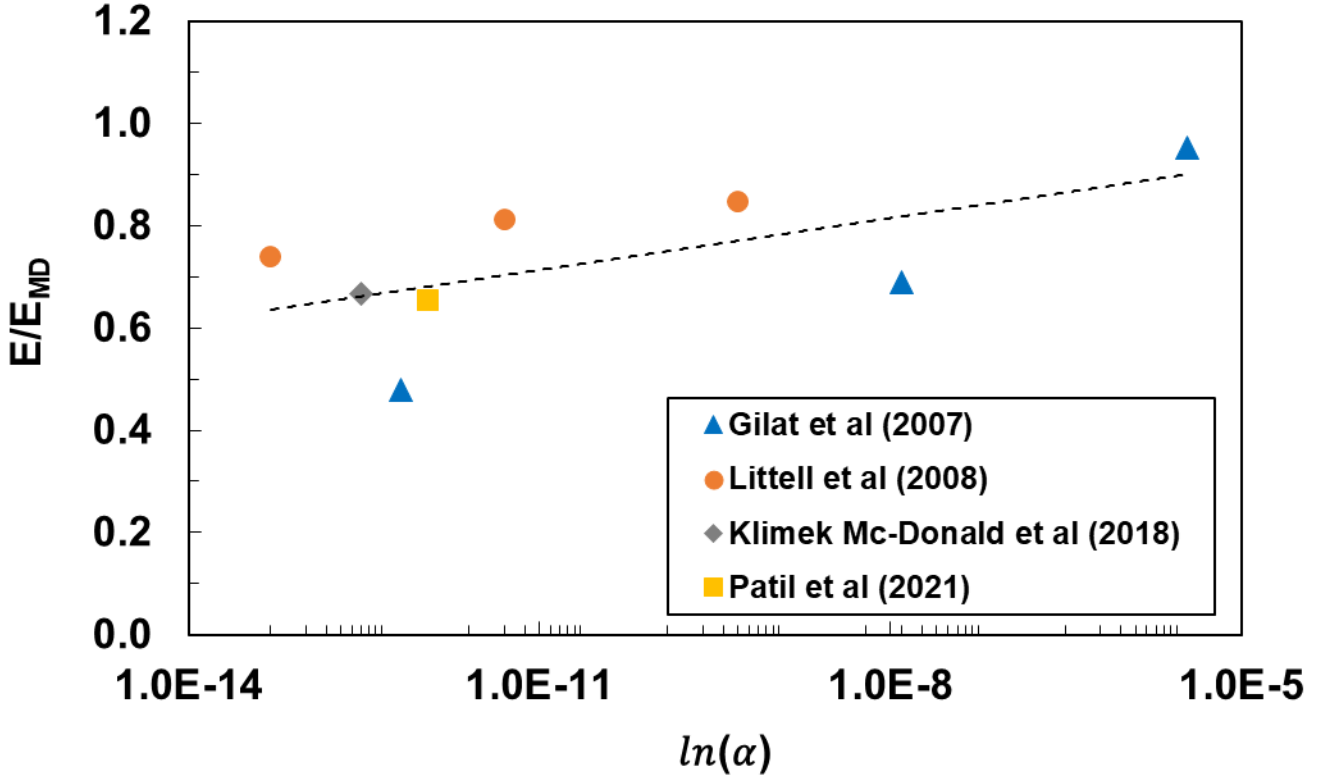
Figure 3 – Normalized Young's modulus of DGEBF/DETDA epoxy as a function of applied normalized strain rate determined experimentally

As shown in Figure 2b, the storage modulus exhibits a sigmoid-type response as a function of degree of cure. Thus, a logical choice for the $f_\phi(\phi)$ functional form is a Fermi-Dirac function [38], whose value ranges between 0 and 1 and describes a continuous, yet step-like change from 0 to 1 centered at ϕ_0 with a step change intensity described by ϕ_σ:

$$f_\phi(\phi) = 1 - \left[1 + e^{\left(\frac{\phi - \phi_0}{\phi_\sigma}\right)}\right]^{-1} \tag{5}$$

Using the data shown in Figure 2b, values of ϕ_0 and ϕ_σ were determined by focusing the center of the sigmoid on the drop in modulus between degrees of cure of 45 and 55%. The corresponding dimensionless values are $\phi_0 = 0.45$ and $\phi_\sigma = 0.02$.

From the data shown in Figure 2a, it is clear that the modulus exhibits a sigmoid-type response with respect to temperature. Furthermore, it is evident that this temperature response is dependent on the degree of cure of the thermoset. Therefore, a functional form of $f_{\tau}(\tau,\phi)$ that captures this dependance is

$$f_{\tau}(\tau, \phi) = \left\{ 1 - \left[1 + e^{\left(\frac{\tau - \tau_0(\phi)}{\tau_\sigma} \right)} \right]^{-1} \right\} \tau_*(\tau) \tag{6}$$

where $\tau_0(\phi)$ corresponds to the center of the sigmoidal-type response associated with the glass transition, which is dependent on ϕ; τ_σ describes the step change intensity of the transition; and $\tau^*(\tau)$ describes the change in the mechanical properties with temperature under the T_g. The value of τ_0 can be described with

$$\tau_0(\phi) = \tau_0{}^a \phi + \tau_0{}^b \tag{7}$$

where $\tau_0{}^a$ and $\tau_0{}^b$ are dimensionless phenomenological parameters. The value of τ_* is described by

$$\tau_*(\tau) = \tau_*{}^a \tau^{(\tau_*{}^b)} \tag{8}$$

where $\tau_*{}^a$ and $\tau_*{}^b$ are dimensionless phenomenological parameters. The parameters in Equations 6, 7, and 8 were determined using the DMA data shown in Figure 2a. The same data is plotted in Figure 4 versus τ for all mixing ratios. The parameters $\tau_0{}^a$ and $\tau_0{}^b$ were determined by locating the sigmoid centers of the data in Figure 4 for the different degrees of cure and fitting those values to the linear function shown in Equation 7. The best-fit values were $\tau_0{}^a = -0.4712$ and $\tau_0{}^b = 0.5268$.

Close examination of Figure 4 shows that the curves do not exactly exhibit a sigmoidal shape, that is, for higher values of τ beyond the center of the sigmoid, the storage modulus continues to increase by a steady amount (modulus is a function of temperature in the glassy regime). Therefore, the τ^* multiplier in Equation 6 is used to correct the sigmoid for this discrepancy. From Figure 4 it is also evident that the maximum value of the modulus for each degree of cure proxy follows the same trend observed in Figure 2b, that is, the maximum value is the greatest for $\phi = 65\%$. Once again, the maximum value of the modulus would be expected to occur at $\phi = 100\%$ if these curves were from epoxies with intermediate degrees of cure, instead of proxies. However, as explained above, the proxy systems were used to characterize Equations 5-8 because of the convenience of obtaining modulus data for a range of degrees of cure and temperature using proxy systems. The values for $\tau_*{}^a$ and $\tau_*{}^b$ were determined by quantifying the discrepancy between the modulus values from the DMA data just above the sigmoidal jump and the modulus of the full stoichiometry system at room temperature. The relationship between these discrepancy values and their corresponding τ values were fit with the power law relationship of Equation 8. The corresponding phenomenological parameters are $\tau_*{}^a = 1.4$ and $\tau_*{}^b = 0.3$.

Finally, with the initial guess values of eight out of nine phenomenological parameters determined, the final parameter, τ_σ, which describes the relative steepness of the sigmoid jumps shown in Figure 4, was determined using a least-squares fit of Equations 3-8 to the DMA data shown in Figure 4, with a value of $\tau_\sigma = 0.009$. The values of the initial guesses are summarized in Table 2.

5.2 Optimization of parameters

After the initial guesses of all the parameters were determined, they were used in the Newton-Raphson iterative optimization technique to determine the final optimized values of the full set of nine parameters. The optimized values are provided in Table 2. Figure 4 shows the storage modulus calculated with Equations 3-8 and the optimized values plotted against the τ parameter. It is important to note that the model predicts the room temperature modulus of each system to be equal to that of the full stoichiometry system. The model parameters were fit this way to offset the effect of using a series of proxy systems instead of fully stoichiometric systems at partial degrees of cure.

Table 2 – Material parameters for the viscous correction (all values are dimensionless)

Phenomenological material parameter	Optimized values
α_a	0.0147
α_b	1.0849
ϕ_0	0.4737
ϕ_σ	0.0263
$\tau_0{}^a$	-0.4739
$\tau_0{}^b$	0.5290
$\tau_*{}^a$	1.3129
$\tau_*{}^b$	0.2375
τ_σ	0.0100
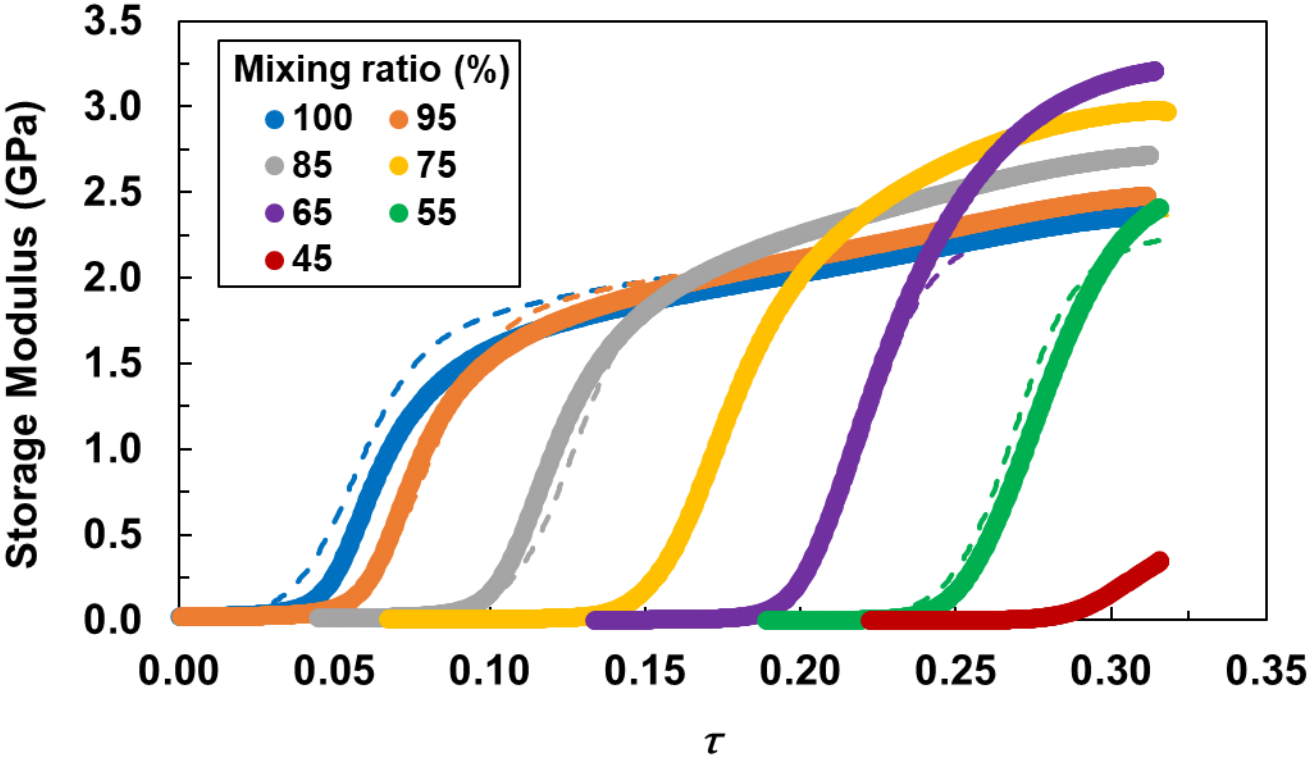
6. Application of correction to MD predictions

It is uncommon for all the crosslinking reactions that can occur in a thermoset network to actually occur because of steric hindrance constrains on the motion of the reactive groups[39, 40]. The degree of cure is defined as the relative amount of conversion that has occurred in a thermosetting polymer system, ranging from 0 (no crosslinking reactions have occurred) to 1.0 (100% of all crosslinking reactions have occurred that can possibly occur given steric hindrance constraints). Conversely, the crosslink density, as defined above, indicates the relative number of crosslinking reactions that have occurred with respect to the total number of reactive group pairs that exist in the material. Therefore, it is typical for a crosslink density to never reach 100%, but a degree of cure can always reach 100% given a sufficiently long cure time. Because the crosslink density is a convenient metric to track with MD, but degree of cure is more convenient from a processing perspective, it is necessary to convert the crosslink densities simulated with MD to degree of cure quantified experimentally. With these definitions, the degree of cure can be determined from the crosslink density as follows:

- The degree of cure is 0 when the crosslink density is 0
- The degree of cure is 1 when the crosslink density has reached its maximum value for a given material
- Intermediate values of the degree of cure are calculated using a linear scaling such that the degree of cure is the ratio of the crosslink density to the maximum crosslink density

MD simulations were reported by Patil et al [8] to predict the Young's modulus of the same DGEBF/DETDA epoxy system studied herein as a function of crosslinking density. In this study, after converting the data of Patil et al to be a function of degree of cure, the correction factor from Equations 3-8 was applied using the optimized parameters shown in Table 2.

The viscous response of thermoset materials is only apparent in deformations with a finite deviatoric (shape changing) component of deformation. For hydrostatic (volume changing) deformations, the response is purely elastic [41]. Therefore, it is possible to predict the viscous response of the Poisson's ratio (v) for the isotropic epoxy system as a function of degree of cure, temperature, and strain rate through the standard elasticity equation

$$v = \frac{3K - E}{6K} \tag{9}$$

Where K is the bulk modulus, which was predicted by Patil et al [8] for this epoxy system as a function of crosslink density. Thus, the Poisson's ratio was determined for a range of degrees of cure at room temperature.

7. Results

Figure 5 shows the corrected MD-predicted Young's modulus for varying temperatures (solid lines) compared with the room temperature MD uncorrected Young's modulus predictions (open circles) with a linear regression fit (dashed line). The experimental data points are included (open diamonds) at varying temperatures, as well as a data point from Littell et al [36] at 80 °C. As expected, the predicted and measured Young's moduli decrease with increasing temperatures and decreasing degrees of cure.

The corrected modulus for the fully crosslinked state ($\phi = 1$) at all temperatures agrees well with the experimental data. The corrected modulus at 80 °C at degrees of cure above the gel point of the DGEBF/DETDA system ($\phi = 0.6$) [8] is slightly higher than the experimental value before it reduces to match the experimental value as the model approaches the fully crosslinked state. This discrepancy, as explained above, is due to the use of proxy materials systems as a substitute for the full stoichiometry epoxy system with intermediate degrees of cure. As the temperature increases, the corrected moduli exhibit improved agreement with the experimental data both below and above gel point. Also, as the temperature approaches 140 °C, the modulus approaches a near zero value as the material advances toward the transition from glassy to rubbery states (shown in Figure 2c, 155 °C). At 177 °C (the processing temperature for this epoxy system), the modulus is expected to reduce to zero because the material is in the rubbery state and unable to sustain any appreciable mechanical load. This behavior is similar to that observed in Figure 2a, where the storage modulus goes to zero at 177 °C.

Perhaps the most striking feature of Figure 5 is the overall significance of the viscous correction on the MD predicted modulus values. Figure 6 shows the overall reduction in the MD predicted modulus as a function of degree of cure and temperature. It can be seen that the correction is highest for low degrees of cure and high temperatures, and lowest for high degrees of cure and low temperatures. Thus, the need for the correction in MD predictions of thermoset properties is clearly evident for not only strain rates, but for temperatures and degrees of cure as well.
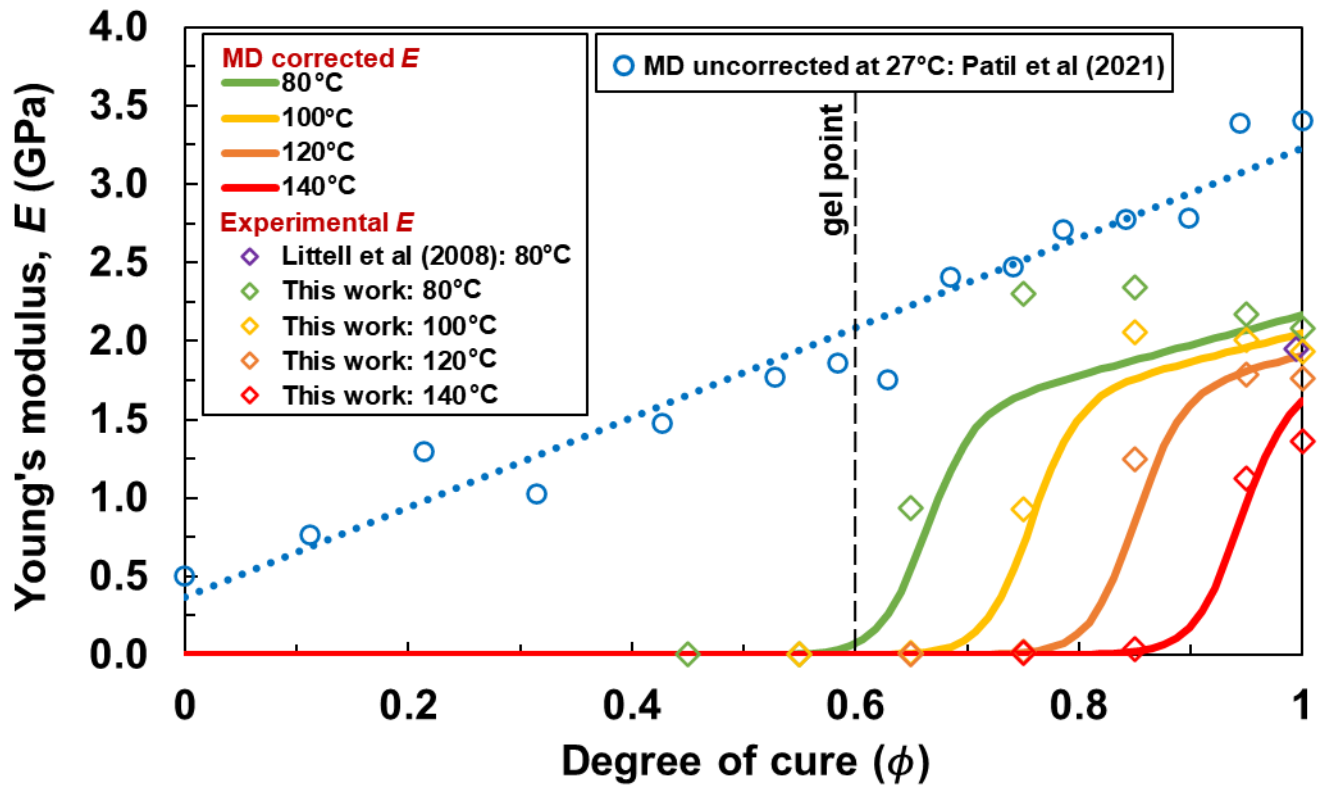
Figure 5– Plot of MD uncorrected (open circles) and corrected (solid lines) Young's modulus vs degree of cure for varying temperatures along with experimental data (open diamonds).
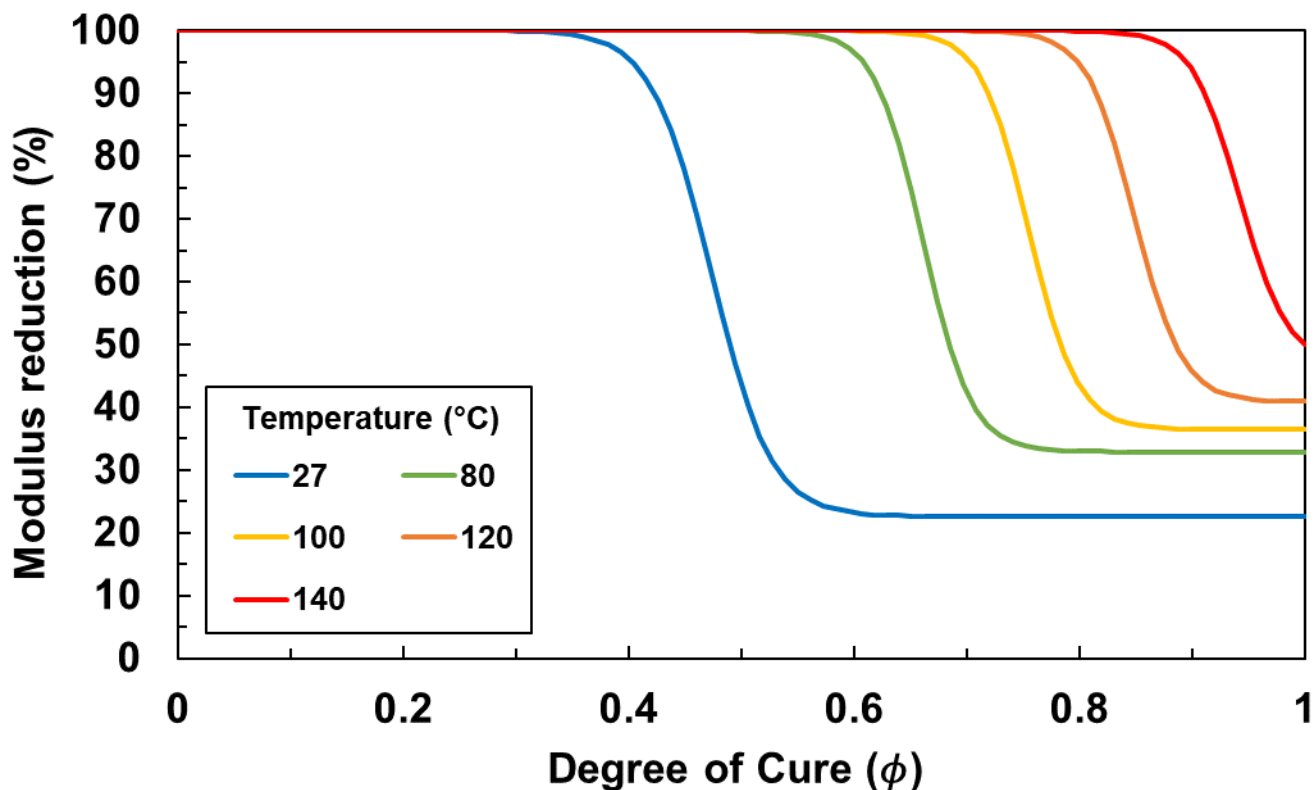
Figure 6– Plot of modulus correction vs degree of cure for varying temperatures.

Figure 7 shows the corrected MD-predicted Poisson's ratio for varying temperatures (solid lines) compared with the room temperature MD uncorrected Poisson's ratio predictions (open blue circles) with a linear regression fit (dashed line). An experimental data point from Littell et al [36] at 80 °C is also included (open diamond). The predicted Poisson's ratio increases with increasing temperatures, in agreement with experiment [42-47], because of increased molecular motion. The predicted Poisson's ratio generally decreases with increasing degrees of cure, as observed experimentally [48, 49].

In the fully cured state ($\phi = 1$), the predicted Poisson's ratios show no significant difference with respect to temperature. Littell et al [36] also observed an insignificant difference in the experimentally measured Poisson's ratio of 0.4, 0.4 and 0.38 at temperatures of 27 °C, 50 °C and 80 °C, respectively, from tensile tests at a strain rate of $1 \times 10^{-1}\,\mathrm{s}^{-1}$.

As the temperature approaches 140 °C (near the T_g, as shown in Figure 2c), the MD-corrected Poisson's ratio approaches an asymptotic value of 0.5, similar to an incompressible liquid. For 177 °C (above the T_g), the Poisson's ratio is expected to reach 0.5 for the entire range of degree of cure. This behavior of the MD-corrected Poisson's ratio with temperature agrees well with experimental observations [45-49].
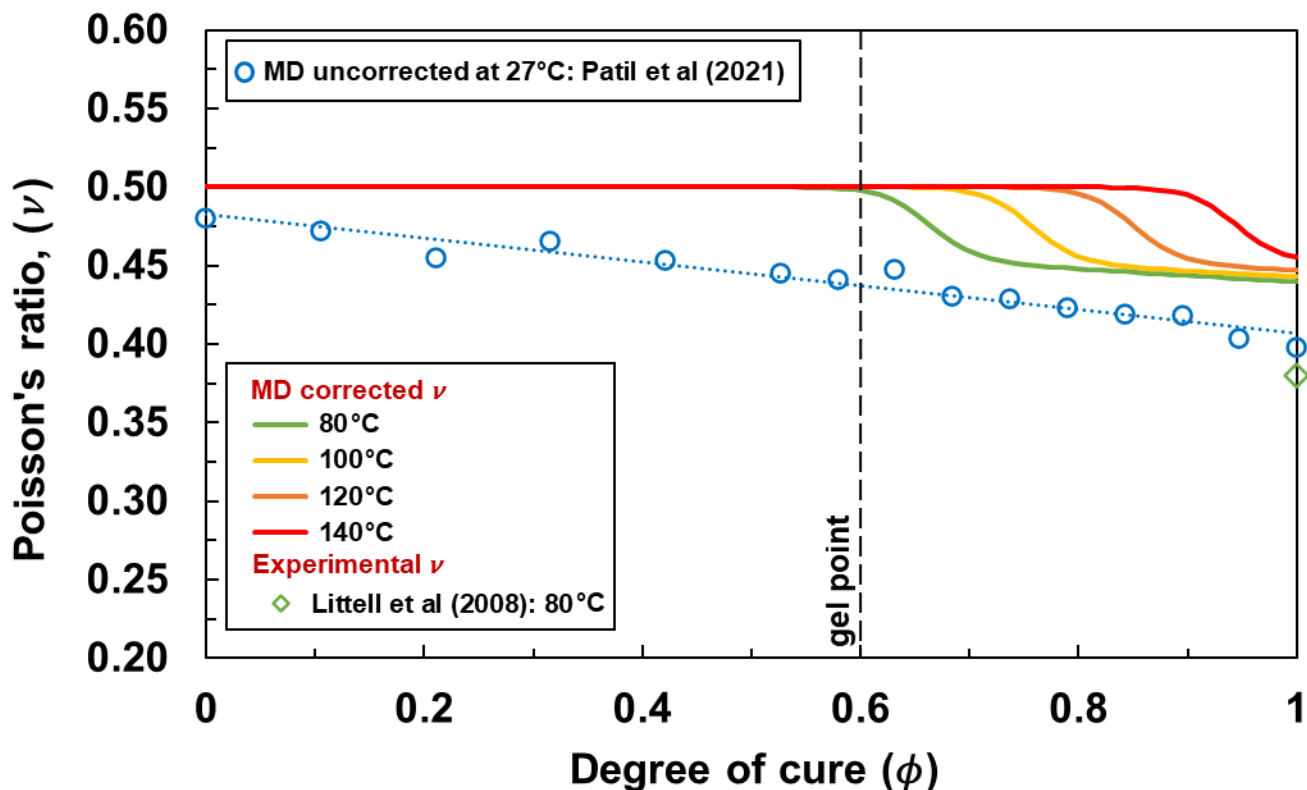
Figure 7– Plot of MD uncorrected (solid circles) and corrected (solid lines) Poisson's ratio vs degree of cure for varying temperatures along with experimental data (solid diamonds).

Conclusions

An efficient phenomenological-based correction factor has been developed for correcting MD-predicted elastic properties of thermosets that exhibit significant viscoelastic effects, such as the DGEBF/DETDA epoxy system studied herein. This approach satisfies the four requirements articulated at the beginning of this study. First, the method requires only minimal MD simulations. Only MD predictions of the mechanical properties of the polymer at multiple degrees of cure are needed, as opposed to an ambitious program of simulations to establish the time-temperature superposition relationship. Second, the method requires minimal experimental input. Only the storage modulus from DMA temperature sweep tests on off-stoichiometry specimens are required, and not the rigorous experimental characterization of the full viscoelastic constitutive response. Third, this approach directly addresses the well-known major issues associated with the inability of all-atom MD to fully simulate conformational relaxation processes at nanosecond timescales. Specifically, the over-estimation of mechanical properties at MD-scale strain rates, at temperatures above T_g, and at intermediate degrees of cure.

It's important to note that this approach is intended for efficient correction of MD-predicted properties of viscoelastic thermosets. This level of efficiency is particularly beneficial for materials engineering environments where computational material design and process optimization need to be performed in a timely manner. This approach is not a direct substitute for comprehensive characterization of viscoelastic constitutive models or complete quantification of properties at intermediate degrees of cure. However, it

14

does offer a simple approach to correct MD simulation data for the strain-rate effect and the overestimation of properties at elevated temperatures and intermediate degrees of cure.

Acknowledgements

Data Availability

The raw/processed data required to reproduce these findings cannot be shared at this time as the data also forms part of an ongoing study.

REFERENCES

1.   Odegard, G.M. and A. Bandyopadhyay, *Physical aging of epoxy polymers and their composites.* Journal of Polymer Science Part B: Polymer Physics, 2011. **49**(24): p. 1695-1716.
2.   Estridge, C.E., *The effects of competitive primary and secondary amine reactivity on the structural evolution and properties of an epoxy thermoset resin during cure: A molecular dynamics study.* Polymer, 2018. **141**: p. 12-20.
3.   Kallivokas, S.V., A.P. Sgouros, and D.N. Theodorou, *Molecular dynamics simulations of EPON-862/DETDA epoxy networks: structure, topology, elastic constants, and local dynamics.* Soft Matter, 2019. **15**(4): p. 721-733.
4.   Li, C. and A. Strachan, *Molecular dynamics predictions of thermal and mechanical properties of thermoset polymer EPON862/DETDA.* Polymer, 2011. **52**(13): p. 2920-2928.
5.   Li, C. and A. Strachan, *Molecular scale simulations on thermoset polymers: A review.* Journal of Polymer Science Part B: Polymer Physics, 2015. **53**(2): p. 103-122.
6.   Odegard, G.M., B.D. Jensen, S. Gowtham, J. Wu, J. He, and Z. Zhang, *Predicting mechanical response of crosslinked epoxy using ReaxFF.* Chemical Physics Letters, 2014. **591**: p. 175-178.
7.   Odegard, G.M., S.U. Patil, P.P. Deshpande, K. Kanhaiya, J.J. Winetrout, H. Heinz, S.P. Shah, and M. Maiaru, *Molecular Dynamics Modeling of Epoxy Resins Using the Reactive Interface Force Field.* Macromolecules, 2021. **54**(21): p. 9815-9824.
8.   Patil, S.U., S.P. Shah, M. Olaya, P.P. Deshpande, M. Maiaru, and G.M. Odegard, *Reactive Molecular Dynamics Simulation of Epoxy for the Full Cross-Linking Process.* ACS Applied Polymer Materials, 2021.
9.   Radue, M.S., B.D. Jensen, S. Gowtham, D.R. Klimek-McDonald, J.A. King, and G.M. Odegard, *Comparing the Mechanical Response of Di-, Tri-, and Tetra-functional Resin Epoxies with Reactive Molecular Dynamics.* J Polym Sci B Polym Phys, 2018. **56**(3): p. 255-264.
10.   Radue, M.S., V. Varshney, J.W. Baur, A.K. Roy, and G.M. Odegard, *Molecular Modeling of Cross-Linked Polymers with Complex Cure Pathways: A Case Study of Bismaleimide Resins.* Macromolecules, 2018. **51**(5): p. 1830-1840.

11. Sirk, T.W., K.S. Khare, M. Karim, J.L. Lenhart, J.W. Andzelm, G.B. McKenna, and R. Khare, *High strain rate mechanical properties of a cross-linked epoxy across the glass transition.* Polymer, 2013. **54**(26): p. 7048-7057.

12. Tsige, M., C.D. Lorenz, and M.J. Stevens, *Role of Network Connectivity on the Mechanical Properties of Highly Cross-Linked Polymers.* Macromolecules, 2004. **37**(22): p. 8466-8472.

13. Varshney, V., S.S. Patnaik, A.K. Roy, and B.L. Farmer, *A Molecular Dynamics Study of Epoxy-Based Networks: Cross-Linking Procedure and Prediction of Molecular and Material Properties.* Macromolecules, 2008. **41**(18): p. 6837-6842.

14. Vashisth, A., C. Ashraf, W. Zhang, C.E. Bakis, and A.C.T. van Duin, *Accelerated ReaxFF Simulations for Describing the Reactive Cross-Linking of Polymers.* J Phys Chem A, 2018. **122**(32): p. 6633-6642.

15. Odegard, G.M., S.U. Patil, P.S. Gaikwad, P. Deshpande, A.S. Krieg, S.P. Shah, A. Reyes, T. Dickens, J.A. King, and M. Maiaru, *Accurate predictions of thermoset resin glass transition temperatures from all-atom molecular dynamics simulation.* Soft Matter, 2022.

16. Aramoon, A., T.D. Breitzman, C. Woodward, and J.A. El-Awady, *Coarse-Grained Molecular Dynamics Study of the Curing and Properties of Highly Cross-Linked Epoxy Polymers.* The Journal of Physical Chemistry B, 2016. **120**(35): p. 9495-9505.

17. Yang, S., Z. Cui, and J. Qu, *A Coarse-Grained Model for Epoxy Molding Compound.* The Journal of Physical Chemistry B, 2014. **118**(6): p. 1660-1669.

18. Langeloth, M., T. Sugii, M.C. Böhm, and F. Müller-Plathe, *The glass transition in cured epoxy thermosets: A comparative molecular dynamics study in coarse-grained and atomistic resolution.* The Journal of Chemical Physics, 2015. **143**(24): p. 243158.

19. Li, C. and A. Strachan, *Coarse-grained molecular dynamics modeling of reaction-induced phase separation.* Polymer, 2018. **149**: p. 30-38.

20. Yang, S. and J. Qu, *Coarse-grained molecular dynamics simulations of the tensile behavior of a thermosetting polymer.* Physical Review E, 2014. **90**(1): p. 012601.

21. Shah, S.P., S.U. Patil, C.J. Hansen, G.M. Odegard, and M. Maiarù, *Process modeling and characterization of thermoset composites for residual stress prediction.* Mechanics of Advanced Materials and Structures, 2021: p. 1-12.

22. Kravchenko, O.G., C. Li, A. Strachan, S.G. Kravchenko, and R.B. Pipes, *Prediction of the chemical and thermal shrinkage in a thermoset polymer.* Composites Part A: Applied Science and Manufacturing, 2014. **66**: p. 35-43.

23. Park, H., J. Choi, B. Kim, S. Yang, H. Shin, and M. Cho, *Toward the constitutive modeling of epoxy matrix: Temperature-accelerated quasi-static molecular simulations consistent with the experimental test.* Composites Part B: Engineering, 2018. **142**: p. 131-141.

24. Park, H. and M. Cho, *A multiscale framework for the elasto-plastic constitutive equations of crosslinked epoxy polymers considering the effects of temperature, strain rate, hydrostatic pressure, and crosslinking density.* Journal of the Mechanics and Physics of Solids, 2020. **142**: p. 103962.

25. Park, C., J. Jung, and G.J. Yun, *Multiscale micromorphic theory compatible with MD simulations in both time-scale and length-scale.* International Journal of Plasticity, 2020. **129**: p. 102680.

26. Park, C., J. Jung, T. Park, and G. Yun, *Multiscale Micromorphic Theory and Simulation with Co-existing Molecular and Continuum Time Scales*, in *AIAA Scitech 2020 Forum*. 2020, American Institute of Aeronautics and Astronautics.

27. Khare, K.S. and F.R. Phelan Jr., *Integration of Atomistic Simulation with Experiment Using Time−Temperature Superposition for a Cross-Linked Epoxy Network.* Macromolecular Theory and Simulations, 2020. **29**(2): p. 1900032.

28. Khare, K.S. and F.R. Phelan, *Quantitative Comparison of Atomistic Simulations with Experiment for a Cross-Linked Epoxy: A Specific Volume–Cooling Rate Analysis.* Macromolecules, 2018. **51**(2): p. 564-575.

29. Olaya, M.N., G.M. Odegard, and M. Maiaru, *A Novel Approach to Characterization of Composite Polymer Matrix Materials for Integrated Computational Materials Engineering Approaches*, in *AIAA Scitech 2021 Forum*.

30. Olaya, M., S. Shah, and M. Maiaru, *Thermoset Polymers Characterization as a Function of Cure State Using Off-Stoichiometry Proxies* in ChemRxiv 2022. This content is a preprint and has not been peer-reviewed.

31. Christensen, R.M., *Chapter I - Viscoelastic Stress Strain Constitutive Relations*, in *Theory of Viscoelasticity (Second Edition)*, R.M. Christensen, Editor. 1982, Academic Press. p. 1-34.

32. *CHAPTER 12 - Nonlinear Viscoelastic Stress Analysis*, in *North-Holland Series in Applied Mathematics and Mechanics*, W.N. Findley, J.S. Lai, and K. Onaran, Editors. 1976, North-Holland. p. 268-288.

33. Buckingham, E., *On Physically Similar Systems; Illustrations of the Use of Dimensional Equations.* Physical Review, 1914. **4**(4): p. 345-376.

34. Galántai, A., *The theory of Newton's method.* Journal of Computational and Applied Mathematics, 2000. **124**(1): p. 25-44.

35. Klimek-McDonald, D.R., J.A. King, I. Miskioglu, E.J. Pineda, and G.M. Odegard, *Determination and Modeling of Mechanical Properties for Graphene Nanoplatelet/Epoxy Composites.* Polymer Composites, 2018. **39**(6): p. 1845-1851.

36. Littell, J.D., C.R. Ruggeri, R.K. Goldberg, G.D. Roberts, W.A. Arnold, and W.K. Binienda, *Measurement of Epoxy Resin Tension, Compression, and Shear Stress–Strain Curves over a Wide Range of Strain Rates Using Small Test Specimens.* Journal of Aerospace Engineering, 2008. **21**(3): p. 162-173.

37. Gilat, A., R.K. Goldberg, and G.D. Roberts, *Strain Rate Sensitivity of Epoxy Resin in Tensile and Shear Loading.* Journal of Aerospace Engineering, 2007. **20**(2): p. 75-89.

38. *Nuts and Bolts of DFT Calculations*, in *Density Functional Theory*. 2009. p. 49-81.

39. Radue, M.S., B.D. Jensen, S. Gowtham, D.R. Klimek-McDonald, J.A. King, and G.M. Odegard, *Comparing the mechanical response of di-, tri-, and tetra-functional resin epoxies with reactive molecular dynamics.* Journal of Polymer Science Part B-Polymer Physics, 2018. **56**(3): p. 255-264.

40. Hadden, C.M., D.R. Klimek-McDonald, E.J. Pineda, J.A. King, A.M. Reichanadter, I. Miskioglu, S. Gowtham, and G.M. Odegard, *Mechanical properties of graphene nanoplatelet/carbon fiber/epoxy hybrid composites: Multiscale modeling and experiments.* Carbon, 2015. **95**: p. 100-112.

41. Flory, P.J., *Principles of polymer chemistry*. 1953: Ithaca : Cornell University Press, 1953.

42. Carneiro, V.H. and H. Puga, *Temperature Variability of Poisson's Ratio and Its Influence on the Complex Modulus Determined by Dynamic Mechanical Analysis.* Technologies, 2018. **6**(3): p. 81.

43. Pandini, S. and A. Pegoretti, *Time, temperature, and strain effects on viscoelastic Poisson's ratio of epoxy resins.* Polymer Engineering & Science, 2008. **48**(7): p. 1434-1441.

44. Migwi, C.M., M.I. Darby, G.H. Wostenholm, B. Yates, M. Moss, and R. Duffy, *A method of determining the shear modulus and Poisson's ratio of polymer materials.* Journal of Materials Science, 1994. **29**(13): p. 3430-3432.

45. Mott, P.H., J.R. Dorgan, and C.M. Roland, *The bulk modulus and Poisson's ratio of "incompressible" materials.* Journal of Sound and Vibration, 2008. **312**(4): p. 572-575.

46. Tcharkhtchi, A., S. Faivre, L.E. Roy, J.P. Trotignon, and J. Verdu, *Mechanical properties of thermosets.* Journal of Materials Science, 1996. **31**(10): p. 2687-2692.

47. Yang, L., L. Yang, and R.L. Lowe, *A viscoelasticity model for polymers: Time, temperature, and hydrostatic pressure dependent Young's modulus and Poisson's ratio across transition temperatures and pressures.* Mechanics of Materials, 2021. **157**: p. 103839.

48. O'Brien, D.J., N.R. Sottos, and S.R. White, *Cure-dependent Viscoelastic Poisson's Ratio of Epoxy.* Experimental Mechanics, 2007. **47**(2): p. 237-249.

49. Saseendran, S., M. Wysocki, and J. Varna, *Cure-state dependent viscoelastic Poisson's ratio of LY5052 epoxy resin.* Advanced Manufacturing: Polymer & Composites Science, 2017. **3**(3): p. 92-100.